Virus Genes (2006) 33:59–68
DOI 10.1007/s11262-005-0030-z

ORIGINAL ARTICLE

The intraleader AUG nucleotide sequence context is important for equine arteritis virus replication

Denis Archambault · Ali Kheyar · Antoine A. F. de Vries · Peter J. M. Rottier

Received: 25 July 2005 / Accepted: 2 November 2005

Abstract The 5′-terminal leader sequence of the equine arteritis virus (EAV) genome contains an open reading frame (ORF) with an AUG codon in a sub-optimal context for initiation of protein synthesis. To investigate the significance of this intraleader ORF (ILO), an expression plasmid was generated carrying a DNA copy of the subgenomic mRNA7 behind a T7 promoter. Capped RNA transcribed from this construct was shown to direct, in an in vitro translation system, the synthesis of leader peptide as well as N protein. Site-directed mutations aimed to either optimize or weaken the sequence context of the ILO start codon affected leader peptide synthesis as predicted; no peptide was detected when the initiation codon was incapacitated. Translation of the downstream N gene was inversely affected by leader peptide production, consistent with a ribosomal leaky scanning mechanism. To investigate the role of the leader peptide in the EAV replication life cycle we generated, using an infectious EAV cDNA clone, two mutant viruses in one of which the ILO start codon was in an optimal Kozak context for translation initiation while in the other the codon was again incapacitated. Surprizingly, both mutant viruses were equally viable and exhibited similar phenotypes in BHK-21 cells. However, their replication kinetics and viral yields were reduced relative to that of the wild-type parental virus, as were their plaque sizes. Importantly, the mutations introduced into the viruses appeared to be rapidly and precisely repaired upon passaging. Already after one viral passage a significant fraction of the viruses had regained the wild-type sequence as well as its phenotype. The results demonstrate that EAV replication is not dependent on the synthesis of the intraleader peptide. Rather, the leader peptide does not seem to have any function in the EAV life cycle. As we discuss, the available data indicate that the ILO 5′ nucleotide sequence per se, not its functioning in translation initiation, is of critical importance for EAV replication.

Keywords Equine arteritis virus (EAV) · Leader peptide · Leader ORF · Translation · Replication

D. Archambault (✉) · A. Kheyar
Department of Biological Sciences,
University of Québec at Montréal, Succursale Centre-Ville,
P.O. Box 8888, H3C 3P8 Montréal, Québec Canada
e-mail: archambault.denis@uqam.ca

A. A. F. de Vries · P. J. M. Rottier
Virology Division, Department of Infectious Diseases and Immunology, Veterinary Faculty, Utrecht University,
Yalelaan 1, 3584 CL, Utrecht, The Netherlands

A. A. F. de Vries
Gene Therapy Section, Department of Molecular Cell Biology, Leiden University Medical Center,
Wassenaarseweg 72, 2333 AL Leiden, The Netherlands

Introduction

Equine arteritis virus (EAV), the aetiologic agent of equine viral arteritis (EVA), is the prototype member of the *Arteriviridae* family, which together with the *Coronaviridae* and *Roniviridae* families constitutes the order Nidovirales [1]. The EAV genome is a positive, single-stranded, 5′-capped and 3′-polyadenylated mRNA molecule with a length of 12,704 nucleotides (nt). During EAV replication, a 3′-coterminal nested

set of seven virus-specific RNAs (RNAs 1 through 7) is produced which direct the synthesis of structural and non-structural viral proteins [2]. Each open reading frame (ORF) in the EAV genome is preceded by the pentanucleotide sequence motif 5′-UCAAC-3′, also called the leader-body junction site [3, 4] or the transcription regulating sequence (TRS) [5]. The TRS motifs, in conjunction with neighboring nt, are key elements involved in the synthesis of the 3′-coterminal nested set of six subgenomic (sg) mRNAs [6, 7] through their fusion, most likely by a discontinuous minus-strand transcription mechanism, with a common leader sequence of 206 nt identical to and derived from the extreme 5′ terminus of the viral genome [8].

We have previously determined the extreme 5′ end of the leader sequence of EAV and reported the presence of an AUG codon at genome positions 14–16 that could open an intraleader ORF (ILO) of 111 nt in length [9]. This ILO was predicted to encode a peptide of 37 amino acids and appeared to be conserved among different EAV isolates [10] which suggested that it may be of functional significance for the virus. Further analysis showed that the ILO start codon was present in a suboptimal context to initiate protein translation, which might explain the efficient translation of the ORFs located downstream of the leader sequence on each EAV mRNA. Because short ORFs within the 5′ leader region of other viral mRNAs have been reported to down-regulate the rate of translation of downstream ORFs [11–13], we hypothesized that the EAV ILO might similarly affect the synthesis of the EAV proteins or have another regulatory function in the life cycle of the virus.

In the present study we performed in vitro transcription and translation experiments to study the expression of the ILO and its effect on the synthesis of EAV N protein. We also studied, by using mutant infectious cDNA clones, the effect of mutations around the ILO AUG codon on the EAV replication.

Materials and methods

Cells, virus and antisera

African green monkey kidney (Vero) and baby hamster kidney (BHK-21) cells were maintained in Dulbecco's modified Eagle's medium (DMEM) supplemented with 10% heat-inactivated fetal bovine serum (FBS) and antibiotics [100 IU/ml of penicillin, 100 μg/ml of streptomycin, and 60 μg/ml of anti-pleuropneumonia-like organisms (PPLO) agent]. The EAV reference Bucyrus strain (ATCC number VR-796) was propagated in cells at a multiplicity of infection (MOI) of 1 [14]. Rabbit antisera directed against bacterial fusion products of the maltose binding protein and the EAV N protein have been described [15]. Antisera against whole EAV and against the leader protein were raised in laboratory rabbits following standard immunization procedures (three antigen inoculations three weeks apart using the Freund's adjuvants with the final bleed 14 days after the last inoculation) using as immunizing antigens a pelleted stock of the Canadian EAV isolate T1329 [10^9 median tissue culture infective dose ($TCID_{50}$) per inoculation] propagated in cell culture [16] and a synthetic peptide (500 μg per inoculation) corresponding to the entire predicted amino acid sequence of the leader protein [9], respectively. The titer of the antiserum raised against the leader peptide was 50,000 as determined in a Western blot assay by using the synthetic peptide as substrate antigen.

RNA extraction and oligonucleotide primers

Total RNA was extracted from 5×10^6 EAV-infected cells with a commercial kit (TRIzol reagent; InVitrogen). The final RNA pellet was dissolved in 30 μl of diethylpyrocarbonate (DEPC)-treated water and stored at −80°C until used. The oligonucleotide primers used in this study are listed in Table 1. They were designed on the basis of the genomic sequence of the Bucyrus reference strain of EAV as determined by Den Boon et al. [4] (GenBank accession number X53459) and Kheyar et al. [10] (GenBank accession number AF001259).

Construction of EAV mRNA7 expression plasmids

Recombinant DNA procedures were adopted from Sambrook et al. [17] or performed according to the instructions supplied with specific reagents. Three microliter of total RNA isolated from the EAV-infected cells at 10 h post-infection (pi) were used as template in a reverse transcription (RT) reaction catalyzed by the avian myeloblastosis virus (AMV) reverse transcriptase (Stratagene). As primer for cDNA synthesis, an oligonucleotide (Peav3′) complementary to the extreme 3′ end of the EAV genomic and sg viral RNAs was used. The cDNA was amplified by the polymerase chain reaction (PCR) using *Pfu* DNA polymerase (Stratagene) and a primer pair consisting of the antisense oligonucleotide Peav3′ and the sense oligonucleotide P(wt)atg which corresponds to the extreme 5′ end of the EAV leader sequence (Table 1). By doing so, we generated a DNA copy of

Table 1 Oligonucleotide primers

Name	Sequence	Polarity	Position [a]
P(wt)atg	5′ *AAGCTTGGATCC***TAATACGACTCACTATA**GCTCGAAGTGTGTATGGTGC 3′	(+)	−29 to 20
P(−)atg	5′ *AAGCTTGGATCC***TAATACGACTCACTATA**GCTCGAAGTGTGTATTGTGC 3′	(+)	−29 to 20
P(opt)atg	5′ *AAGCTTGGATCC***TAATACGACTCACTATA**GCTCGAAGTGAGTATGGTGC 3′	(+)	−29 to 20
P(nf)atg	5′ *AAGCTTGGATCC***TAATACGACTCACTATA**GCTCGAAGTGTGTATGTTGC 3′	(+)	−29 to 20
P(koz)atg	5′ *AAGCTTGGATCC***TAATACGACTCACTATA**GCTCGAAGCCACCATGGTGC 3′	(+)	−29 to 20
Peav3′	5′ ATC*GAATTCGTCGAC*TTTTTTTTTTTTTTTTGGTTCCTGGGTGGC 3′	(−)	12704–12691[b]
PT7(wt)atg	5′ caa*GCGGCCGCGGTACC***TAATACGACTCACTATA**GCTCGAAGTGTGTATGGTGC 3′	(+)	−34 to 20
PT7(ko)atg	5′ caa*GCGGCCGCGGTACC***TAATACGACTCACTATA**GCTCGAAGTGTGTATTGTGC 3′	(+)	−34 to 20
PT7(opt)atg	5′ caa*GCGGCCGCGGTACC***TAATACGACTCACTATA**GCTCGAAGTGAGTATGGTGC 3′	(+)	−34 to 20
P962	5′ AGGACCAGTCTGCTTCAGAG 3′	(−)	981–962
Peav5′	5′ *AAGCTTGGATCC*GCTCGAAGTG 3′	(+)	−12 to 10
P182	5′ ACC CGT CAA GCC ACA AGA TG 3′	(−)	182–163

[a] According to Genbank accession number X53459 adjusted after the addition of 17 nt at the 5′ end of the EAV genome

[b] Exclusive of the oligo (T) trail. These positions do not include the poly T sequence. Italicized capitals refer to recognition sites for the restriction enzymes *Hin*dIII, *Bam*HI, *Eco*RI, *Sal*I, *Not*I and *Kpn*I. Bolded capitals represent T7 RNA polymerase promoter sequences; normal capitals refer to EAV genomic sequences; underlined capitals correspond to the start codon of the ILO ORF with surrounding nucleotides. Lower case letters refer to pBR322 specific nucleotides

EAV mRNA7 downstream of the bacteriophage T7 RNA polymerase promoter, which was introduced by the sense primer. After agarose gel purification, the RNA7-specific DNA fragment was cut with *Bam*HI and *Sal*I and ligated into *Bam*HI- and *Sal*I-digested plasmid vector pUC18 (InVitrogen). The resulting plasmid, designated F7wtATG, was sequenced to verify the correctness of the cloned fragment. As shown in Fig. 1, this construct would theoretically give rise to a RNA transcript of 674 nt in length containing the entire EAV mRNA7 including a 15-A tail.

The construct F7wtATG was used as a template to introduce point mutations in order to modify the sequence context of the ILO initiation codon. PCRs were carried out under the same conditions as described above except that oligonucleotide P(wt)atg was replaced with primer P(−)atg, P(nf)atg, P(opt)atg, or P(koz)atg (Table 1). As a consequence, the generated PCR products lacked an ILO start codon, or contained an IL initiation codon in a highly unfavorable, improved, or optimal context for protein translation initiation [13], respectively. The mutated PCR products were inserted into pUC18 to generate the F7(−)ATG, F7(nf)ATG, F7(opt)ATG, and F7(koz)ATG constructs (Fig. 1). All these constructs were subjected to sequence analysis to confirm the introduced mutations.

In vitro RNA transcription, translation and radioimmunoprecipitation

Plasmid DNA of the aforementioned constructs was prepared by the alkaline lysis method, linearized with

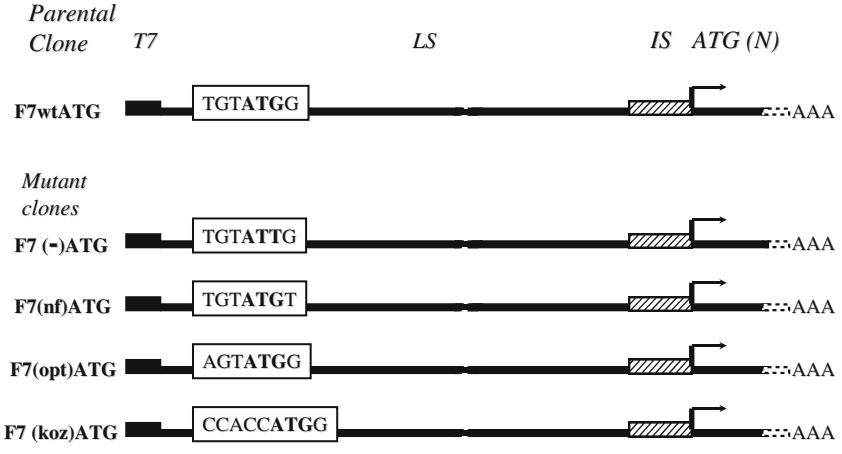

Fig. 1 Schematic representation of the EAV mRNA7-specific plasmid and its derivatives. The parental cDNA clone was generated by RT-PCR and inserted into pUC18 as described in Materials and methods. Indicated are, going from 5′ to 3′: the T7 RNA polymerase promoter sequence (T7, black box), the leader sequence (LS, large black line) containing the ILO start codon with the desired point mutations as indicated (capitals in open box), the intergenic sequence (IS) between the leader sequence, the nucleocapsid start codon (ATG[N]), and the poly(A) tail

*Sal*I, and purified. In vitro transcription experiments were performed with 2-μg template DNA in a 50 μl reaction volume for at 37°C by using a T7 transcription kit (Promega). Cap analogue of type 0 (7 mG(5′) ppp(5′)G) (5 mM) was included during the transcription reaction. The yield and integrity of the RNAs was analyzed by denaturing agarose gel electrophoresis [17] and the concentration of each RNA was estimated by densitometric scanning. In vitro translation was performed with 2 μg of each template RNA in a 50-μl translation mixture by using a reticulocyte lysate system (GE Healthcare). A volume of 5 μl of each sample was loaded onto a sodium dodecyl sulfate (SDS)–15% polyacrylamide (PAA) gel. After electrophoresis, the gels were fixed in 10% acetic acid–50% methanol for 30 min, impregnated with a scintillant (En^{3}hance^{TM}, Dupont) for 30 min, washed 3 times in water, dried, and exposed for 6 h using an X-OMAT AR-5 film (Eastman Kodak). Fluorograms were subsequently analyzed by densitometry to measure the effects of each mutation on N synthesis.

The specificity of the in vitro translated products was analyzed by radioimmunoprecipitation assay (RIPA) [18] by using the appropriate rabbit sera. The RIPA samples were analyzed in SDS–15% PAA gels. The gels were processed as described above and subjected to densitometrical analysis for protein quantitation.

Generation of full-length EAV cDNA clones with mutations in the EAV leader sequence

The construction of the full-length EAV cDNA pBRNX1.038 has been described previously [19]. In this pBR322-based construct, the genomic sequence of the Utrecht variant of the Bucyrus strain of EAV is preceded by a bacteriophage SP6 RNA polymerase promoter. To generate three new EAV cDNA clones, a series of PCRs was performed by using plasmid pBRNX1.038 as a template, the ORF 1a-specific oligonucleotide P962 as an antisense primer, and the leader-specific oligonucleotides PT7(wt)atg, PT7(ko)atg, or PT7(opt)atg as alternative sense primers (Table 1). The resulting PCR products were digested with *Not*I and *Apo*I and stored as fragments of 897 nt in length until used. Another aliquot of plasmid pBRNX1.038 was digested with the unique restriction enzymes *Not*I and *Eco*RV, which generates fragments of 12,672 and 4,282 nt, respectively. The small fragment, which contained the SP6 promoter sequence and the wild-type ILO start codon, was purified from the gel and digested with *Apo*I to obtain a 891-nt *Not*I–*Apo*I fragment and a 3391-nt *Apo*I–*Eco*RV fragment. The latter DNA fragment was gel-purified and stored until further use. It is noteworthy that there was a 6 nt difference in length between the *Not*I–*Apo*I fragments generated by PCR and the *Not*I–*Apo*I fragment obtained by digestion of plasmid pBRNX1.038. This difference is due to the insertion of a *Kpn*I site between the *Not*I site and the T7 promoter sequence in primers PT7(wt)atg, PT7(ko)atg and PT7(opt)atg (Table 1). The additional *Kpn*I site allowed us to distinguish, by restriction enzyme analysis, the original SP6 promoter-containing infectious cDNA clone pBRNX1.038 from the newly generated T7 promoter-containing full-length EAV cDNA clones.

Each of the *Not*I- and *Apo*I-digested PCR products was dephosphorylated by using the calf intestinal alkaline phosphatase (GE Healthcare) and ligated to the 3391-nt *Apo*I–*Eco*RV fragment of plasmid pBRNX1.038 to generate *Not*I–*Eco*RV fragments of 4,288 bp in length. These fragments were gel-purified and ligated to the 12,672-nt *Eco*RV–*Not*I fragment of pBRNX1.038 to generate the T7NX(wt)ATG wild-type full-length cDNA clone and the two mutant full-length cDNA clones T7NX(ko)ATG and T7NX(opt)ATG. Each of these constructs was used to transform *E. coli* UltraMax DH5α (InVitrogen) cells. Finally, the resulting plasmids were sequenced in the leader region by using primer P182.

It is acknowledged that these clones might have contained unintended mutations elsewhere in the viral genome introduced during genetic manipulation. Thus, to ensure that any phenotypic difference between wild-type EAV and the mutant viruses was indeed the result of the point mutations introduced in the vicinity of the ILO start codon, we restored the wild-type genotype in the mutant full-length EAV cDNA clones. For this purpose, oligonucleotide PT7(wt)atg containing the wild-type ILO initiation codon was used as the sense primer and oligonucleotide P962 as the antisense primer (Table 1). To reconstruct full-length cDNA clones that would include these newly generated PCR fragments, we used the same procedure as described above and derived all remaining sequences from the plasmids that were subjected to restoration, i.e. T7NX(ko)ATG and T7NX(opt)ATG. The resulting constructs were designated T7NX(ko-to-wt)ATG and T7NX(opt-to-wt)ATG to indicate restoration of the ILO translational start site.

RNA transfection of cells and recovery of recombinant viruses

Capped run-off RNA transcripts from the *Xho*I linearized EAV cDNA clones T7NX(wt)ATG, T7NX(ko)ATG, T7NX(opt)ATG, T7NX(ko-to-wt)

ATG, and T7NX(opt-to-wt)ATG were prepared by using the MEGAscript transcription kit (Ambion).

RNA transcripts (10–20 μg), whose integrity was verified by denaturing agarose gel electrophoresis prior to cell transfection, were transfected into subconfluent monolayers of BHK-21 cells by electroporation (carried out at room temperature or on ice-water with two consecutive pulses of 300 V, low R ohms (4,000 Ω), 60 μF) by using the Cell-Porator™ electroporation system (InVitrogen). In certain samples, RSV-*β*-galactosidase plasmid (1 μg) was used as a control for transfection efficiency. The cells were then seeded in 25-cm^2 tissue culture flasks until observation of typical EAV cytopathic effect (CPE). Recombinant viruses were harvested essentially as previously described [14].

Serial passage and genetic analysis of recombinant viruses

To study the stability of the introduced mutations, the recombinant viruses recEAV(ko)AUG and recEAV(opt)AUG were serially propagated in BHK-21 cells until the 15th passage and collected at each passage when 80–90% of the cells exhibited a CPE [14]. Virus-containing supernatants from transfected cells (passage P0) and from viral passages 5, 10 and 15 were analyzed for the presence of the introduced point mutations by RT-PCR sequencing. Primers used in the PCR were the sense Peav5′ primer (corresponding to the first 10 nt at the 5′ end of the EAV leader sequence) and the antisense P182 primer (Table 1). The PCR products (from two independent reactions) were then sequenced through the McGill University (Montreal) sequencing services.

Growth curves and plaque assay

BHK-21 cell monolayers in 6-well tissue culture plates were infected with each of the recombinant viruses (one well per recombinant virus) at an MOI of 0.5. At various times pi, the cell cultures were subjected to three cycles of freezing and thawing. The cell lysates were then clarified by centrifugation for 15 min at 5000*g* and the viral titer ($TCID_{50}$ per milliliter) of the supernatants was determined as previously described [14].

Plaque assay was performed with virus samples collected from transfected cells (P0) and from viral passage 15 (P15) in order to compare the morphology and size of plaques of the viruses recEAV(ko)AUG and recEAV(opt)AUG with those of recombinant wild-type EAV. The virus samples were diluted to such an extent that one 10-cm^2 cell culture dish contained 10–100 plaques. The plaque assay was carried out following standard procedures [20].

Results

In vitro expression and significance of the EAV intraleader peptide

Computer analysis [21] predicted that the IL peptide contained at least one linear epitope. Accordingly, we were able to successfully generate a rabbit antiserum directed against a synthetic version of the protein. However, with this serum, we failed to detect the IL peptide in EAV-infected cells either by immunofluorescence, or by Western blot, or by RIPA (data not shown). We next generated a plasmid (F7wtATG) containing the EAV mRNA7 sequence downstream of a bacteriophage T7 RNA polymerase promoter. In vitro transcripts derived from F7wtATG were translated in vitro and the translation products were directly analyzed by SDS-PAGE. As shown in Fig. 2a (lane 1), polypeptide species of 14 and 4 kDa were detected corresponding to the N protein and the IL peptide, respectively. This result demonstrates that EAV mRNA7 is functionally bicistronic. Because the ILO start codon present in this wild-type construct is in the suboptimal context for translation initiation (13), we

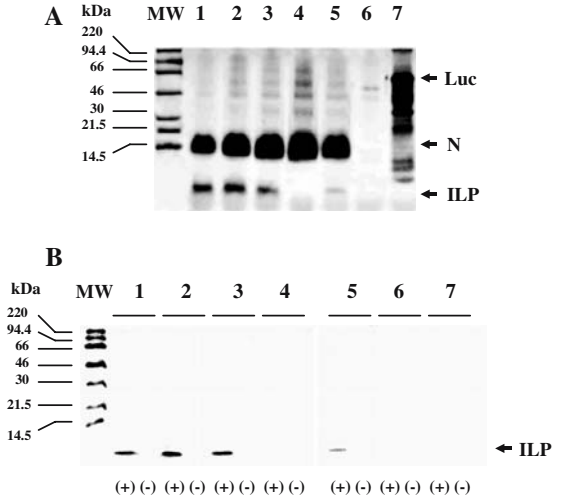

Fig. 2 In vitro synthesis of the EAV IL peptide and N protein. (**A**) Direct visualization of [^{35}S] methionine-labeled in vitro translation products in tricine-buffered SDS–10% PAA gels. The transcripts used for in vitro translation were derived from F7(wt)ATG (lane 1), F7(koz)ATG (lane 2), F7(opt)ATG (lane 3), F7(−)ATG (lane 4) and F7(nf)ATG (lane 5). Lanes 6 and 7 show the result of in vitro translation reactions without RNA (negative control) and with a transcript encoding the luciferase (Luc) protein (positive control), respectively. The positions of the IL peptide (ILP) and the nucleocapsid protein (N) are indicated. (**B**) RIPA of the EAV IL peptide synthesized in vitro using a rabbit antiserum specific for the IL peptide (+) or the corresponding preimmune serum (−) The lane number assignments are the same as in panel A. [^{14}C]-labeled molecular weight (MW) standards (kDa) (GE Healthcare) are indicated at the left

decided to introduce point mutations at the 5′ end of the ILO to improve or abrogate its translation. As shown in Fig. 2a (lanes 2 and 3), the IL peptides from mutant plasmids F7(koz)ATG and F7(opt)ATG (in which the context of the ILO initiation codon was improved) were detected at levels comparable to that of the wild-type construct. As expected, lower amounts of the IL peptide were obtained with the construct F7(nf)ATG which had the ILO AUG codon placed in an unfavorable context for initiation of translation (Fig. 2a, lane 5). No translation product was observed from the mutant clone F7(−)ATG in which the ILO initiation codon was abrogated (Fig. 2a, lane 4). To confirm that the 4 kDa translation product is encoded by the ILO, RIPAs were performed using the rabbit anti-IL peptide serum or the corresponding preimmune serum (Fig. 2b). This experiment proved that the 4 kDa protein is encoded by the ILO and corroborated the previous finding that the amount of IL peptide synthesized depends on the context of the ILO start codon.

We next analyzed the effect of the mutations around the ILO start codon on the production of the N protein. As shown in Fig. 3, an approximately two-fold increase (as determined by densitometric analysis) in the amount of N protein was observed with the mutant constructs F7(−)ATG (lane 2) or F7(nf)ATG (lane 3) relative to that of the wild-type plasmid F7(wt)ATG (lane 1). In contrast, slightly diminished N protein

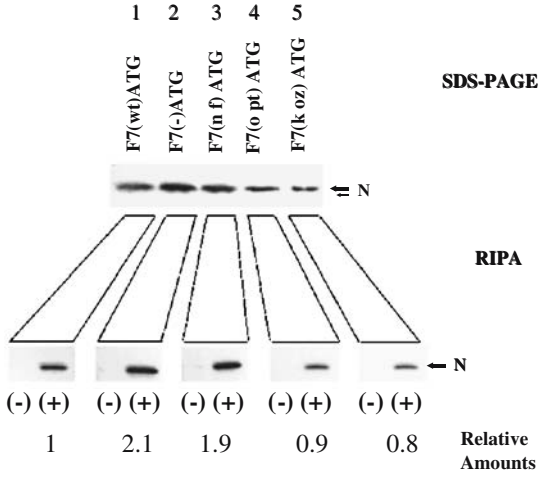

Fig. 3 Effect of the ILO start codon and its direct surroundings on the in vitro translation of the EAV N protein. In vitro translation products of the mRNA7 expression plasmids [F7(wt)ATG, F7(−)ATG, F7(nf)ATG, F7(opt)ATG, and F7(koz)ATG; lanes 1–5, respectively] were analyzed directly by SDS-PAGE and after immunoprecipitation (RIPA) using a rabbit antiserum raised against the EAV N protein (+) or the corresponding preimmune serum (−). The mean relative amounts of N protein were calculated from both experiments and for each construct and normalized to the parental construct (F7(wt)ATG) as indicated at the bottom

levels (15–20% less) were obtained with in vitro transcripts from the mutant clones F7(opt)ATG and F7(koz)ATG (lanes 4 and 5, respectively). Thus, we concluded that translation of the ILO has a negative effect on N protein synthesis. These results are suggestive of a leaky scanning mechanism [13] for translation of the ORF immediately downstream of the EAV leader sequence in each viral (sg) mRNA.

Infectivity and analysis of recombinant virus growth

Transfection of cells with RNA transcripts derived from the mutant full-length EAV cDNA clones, resulted in the production of infectious virus as determined by the appearance of CPE and our ability to further propagate the virus in cell culture. We studied the growth properties of the viruses derived from the transfected cells (P0). As indicated by their growth curves (Fig. 4), both virus mutants replicated less efficiently than the recombinant wild-type virus. This resulted in more than 10-fold lower viral titers as measured during the period of 14–24/26 h pi and to lower N and M protein synthesis levels at 12, 16, and 18 h pi (data not shown). In contrast, the growth curves of viruses in which the wild-type leader sequence had been restored by genetic manipulation (recEAV[ko-to-wt]AUG-P0 and recEAV[opt-to-wt)AUG-P0) or by repeated passage (recEAV[ko]AUG-P15 and recEAV[opt]AUG-P15) were similar to that of the recombinant wild-type virus.

Genetic stability of mutated recombinant viruses

In order to determine the genetic stability of the mutations introduced in the EAV leader region, the mutant viruses (recEAV[ko]AUG and recEAV[opt]AUG), as well as virus derived from the wild-type EAV cDNA clone (recEAV[wt]AUG), were each passaged fifteen times. EAV RNA was isolated from supernatants of transfected cells (P0) and from supernatants taken after passages P5, P10 and P15 and used for RT-PCR to amplify the 5′ 182 nt of the viral genomes by using the high-fidelity *Pfu* polymerase. The PCR products were sequenced. Surprizingly, both mutants had reverted to the wild-type sequence. Already within five passages, the knock-out mutation had been restored while this took some ten to fifteen passages for the virus carrying the optimized ILO start codon (not shown). These results indicated that both recombinant virus mutants are subject to selective genetic pressure under which viruses acquiring the wild-type sequence around the ILO start codon have a

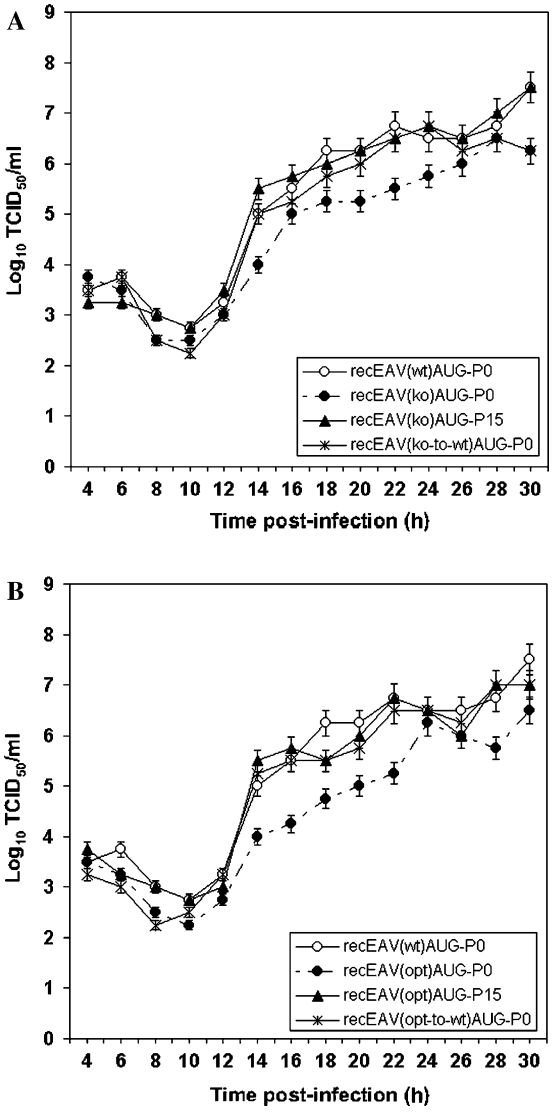

Fig. 4 Growth curves of the EAV recombinant viruses collected after cell transfection (P0) or at the fifteenth viral passage (P15). (**A**) Comparison of growth kinetics of the virus in which the ILO start codon was knocked out (recEAV[ko]AUG-P0) with those of the recombinant wild-type virus (recEAV[wt]AUG-P0) and recombinant viruses in which the wild-type leader sequence was restored by genetic manipulation (recEAV[ko-to-wt]AUG-P0) or by repeated passages (recEAV[ko]AUG-P15). (**B**) Comparison of growth kinetics of the virus in which the context of the ILO start codon was improved (recEAV[opt]AUG-P0) with those of the recombinant wild-type virus (recEAV[wt]AUG-P0) and recombinant viruses in which the wild-type leader sequence was restored by genetic manipulation (recEAV[opt-to-wt]AUG-P0) or by repeated passages (recEAV[opt]AUG-P15). The results are expressed as the mean titers (three independent experiments) ± SD

selective advantage. Consistently, the leader sequence of the wild-type virus appeared to be genetically stable.

Characterization of plaque formation

To further characterize the recombinant mutant viruses, we assessed the size and morphology of their plaques induced in Vero cells after different passages. As shown in Fig. 5, the recombinant wild-type virus (recEAV[wt]AUG-P0) (panel G) yielded a homogeneous population of large plaques with an average diameter of 5 mm. The size and morphology of these plaques were similar to those of the recombinant viruses recEAV(ko-to-wt)AUG-P0 (panel C) and recEAV(opt-to-wt)AUG-P0 (panel F) and to those of the Bucyrus strain of EAV (panel I) which were used as controls. In contrast, plaques of variable size were obtained for the mutant viruses recEAV(ko)AUG-P0 (panel A) and recEAV(opt)AUG-P0 (panel D). It is important to note that most of these plaques (>70%) had an average diameter of about 1.5 mm. However, this heterogeneous plaque phenotype was no longer observed after cell passage 15 (see panels B and E). At this stage, the plaque phenotype had become identical to that of the recombinant viruses with a wild-type leader sequence.

The differences observed in plaque morphology and size prompted us to analyze further the genotype of the virus found in each type of plaque. To this end, total cellular RNA was extracted from individual plaques and used to amplify the leader region by RT-PCR. The PCR products were then sequenced. The results showed that the small plaques were produced by the mutant viruses whereas the medium-size and large plaques contained viruses in which the ILO translation start site had reverted to the wild-type sequence. These

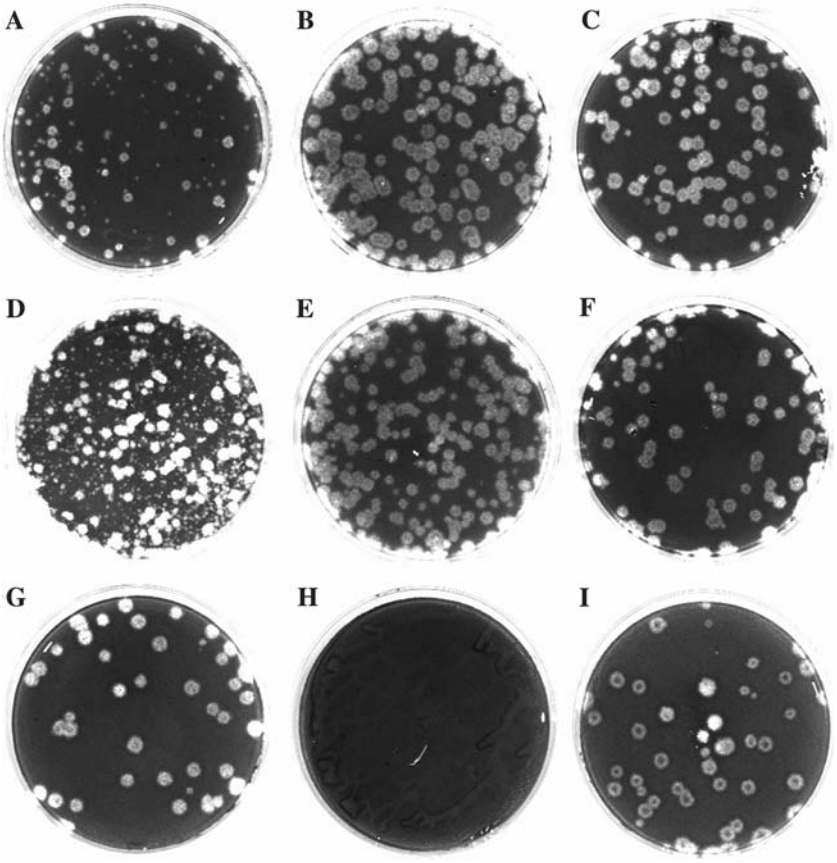

Fig. 5 Plaque morphology of EAV recombinant viruses. Monolayers of Vero cells were infected with recombinant viruses recEAV[ko]AUG-P0 (**A**), recEAV[ko]AUG-P15 (**B**), recEAV[ko-to-wt]AUG-P0 (**C**), recEAV[opt]AUG-P0 (**D**), recEAV[opt]AUG-P15 (**E**), recEAV[opt-to-wt]AUG-P0 (**F**), or recEAV[wt]AUG-P0 (**G**), collected after cell transfection (P0) or at the fifteenth viral passage (P15), or mock-infected (negative control) (**H**) or infected with the Bucyrus strain of EAV (positive control) (**I**), and covered with an agar overlay. At 4 days pi, the overlay was removed and the monolayers were fixed and stained with 0.9% violet crystal in 25% formaldehyde and 5% ethanol

results indicate that restoration of the wild-type genotype had occurred already early during propagation of the mutant viruses and correlated with the observation that plaques of both sizes appeared with both virus mutants following cell transfection.

Discussion

An intraleader ORF occurs in various EAV isolates. Because all genomic and subgenomic viral mRNAs in EAV-infected cells carry the ILO as a consequence of the particular viral replication strategy, a putative role in the EAV life cycle has been suggested [10]. Here we show that the EAV IL peptide is expressed in an in vitro cell-free translation system programmed with a synthetic mRNA7. Hence, we were quite surprized not being able to detect the EAV IL peptide in infected cells despite the mRNA7 abundance, neither by RIPA nor by Western blotting or immunofluoresence assay. This negative result can be explained in a number of ways. First, the IL peptide might simply not be produced during virus replication or be synthesized in very low amounts. Second, the folding of the IL peptide in a reticulocyte lysate may be different from that in virus-infected cells and may hence interfere with its detection. Third, the IL peptide might be rapidly degraded in cells, which would be consistent with our inability to detect the protein by expression from the plasmid using the vaccinia virus vTF7-3 expression system, while synthesis of N protein from this plasmid was clearly observed (data not shown).

Bi- and multicistronic mRNAs occur—though rarely—in normal eukaryotic cells [22] but they appear more frequently among viral mRNAs. Expression of the different genes is regulated by particular sequence conditions. Unless driven by an internal ribosome entry site (IRES), the expression of a downstream ORF is generally inefficient. Accordingly, the in vitro expression of N protein was reduced when the EAV ILO initiation codon was functional, suggestive of a leaky scanning mechanism and consistent with the reported IRES-independent mechanism of translation of EAV mRNAs [7]. The significance, however, of such an attenuating effect of the ILO on the expression of all EAV genes is as yet hard to understand. Also for the related coronaviruses, which are generally devoid of an intraleader ORF, short ILO's have been described [11, 12] but their translation products have never been detected.

Interestingly, the leader peptide per se is not essential for the EAV replication cycle. When we blocked the

expression of the ILO, the mutant virus was able to produce infectious virions, consistent with an earlier study [23] showing EAV infectivity to be maintained after disruption of the intraleader AUG codon. However, unlike this study, modulating the ILO translation efficiency, either positively or negatively, by mutation of the AUG codon or of its context sequence, significantly affected viral characteristics. Mutations that had been confirmed in vitro to either block or enhance the expression of the ILO both resulted in viruses that exhibited delayed growth kinetics, reduced virus yields and smaller plaque size. These mutations appeared to be rapidly restored during serial passages of the viruses. Already during the first cycle a significant fraction of both mutant viruses had reverted to the wild-type phenotype and this effect became progressively complete following subsequent rounds of infection. Phenotypic restoration indeed correlated with genetic correction of the mutations as demonstrated by sequencing.

We can only speculate about the function of the IL peptide in the EAV replication cycle. Either the peptide has no function at all or, though not essential, it does play some subtle role. In the latter case one might envision that a certain, delicate level of the peptide is required for optimal replication. The amount of peptide synthesized would be regulated precisely by the particular sequence context of the initiating AUG. This context would understandably be suboptimal as the efficient expression of the ILO would, through its negative effect on downstream ORFs, be at the unfavorable expense of the synthesis of all other viral proteins. The rapid repair of the mutations that we introduced in and around the AUG sequence would also be consistent with the requirement for a dosed translation of the ILO. What functions the translation product would serve remains as yet unknown. In the alternative interpretation, the IL peptide per se is irrelevant. In that case, it must be the nucleotide sequence at and around the AUG that is of importance.

It has been reported that a 68 nt sequence within the antileader sequence of simian hemorrhagic fever virus (SHFV), another arterivirus, constitutes the specific binding site of four cellular proteins [24]. Cellular proteins appeared to bind to similar regions in the antileader of other arteriviruses including EAV, an observation that we recently confirmed [25]. In addition, we also observed cellular proteins to bind to the EAV leader RNA positive strand and showed that nt 140–206 are not necessary for this binding. Hence, in addition to the base pairing in the vicinity of the leader TRS required for viral transcription, other key functions important in the EAV life cycle appear to reside in the 5′ region of the leader sequence, and the ILO sequence might be one of these. Whether the cellular proteins bind to the ILO, and more particularly to the region carrying the AUG sequence, has yet to be determined. As was done for the 68 nt sequence of SHFV to which cellular protein binds [24], we [10] and others [6] predicted secondary structures in the 5′ genomic region of several EAV isolates. It appears that the ILO AUG codon occurs in a stem-loop structure, base pairing with nucleotides at positions 38–40. By using the *Mfold version 3.1* software of Zuker et al. [26] to predict the secondary structures, the G-to-T mutation introduced in the EAV leader sequence leads to the formation of a small internal loop and a small bulge downstream and in front of the mutation site, respectively. However, the T-to-A mutation leads to the formation of a small internal loop at the mutation site. Whether these secondary structures in the vicinity of the ILO AUG play a role in interactions between the viral RNA and cellular proteins remain to be investigated.

In general, 5′- and 3′-terminal domains of RNA virus genomes play essential roles in replication, transcription and translation. Their sequences are important for recognition by viral and host cell proteins that mediate these processes. In nidovirus replication, the 3′-terminal sequences of the minus strand RNAs, i.e. the sequences complementary to the leader, direct the synthesis of genomic and subgenomic RNAs. It is thus quite plausible that strong selective pressures exist to maintain these sequences. The precision with which the G-to-T mutation in the ILO AUG and the T-to-A mutation at position -3 were repaired supports this view, as does the apparent instability of the reported A-to-G mutation in the AUG [23]. The latter mutation had an identical effect (i.e. complete inhibition) on the expression of the ILO as had our G-to-T mutation. Yet, in contrast to our results, viral replication efficiency nor plaque size were significantly affected. We therefore favor the idea that the IL peptide has no functional significance but that it is the precise nucleotide sequence that is essential for the life cycle of the virus.

Acknowledgements This work was supported by a Discovery operating grant from the National Sciences and Engineering Research Council of Canada to D. Archambault. A. Kheyar was supported by a graduate student fellowship from Université de Montréal. D. Archambault was supported by a senior research scholarship from the Fonds de la Recherche en Santé du Québec.

References

1. D. Cavanagh Arch. Virol. **142**, 629–633 (1997)
2. A. A. F. De Vries, M. C. Horzinek, P. J. M. Rottier, J. R. de Groot Seminars Virol. **8**, 33–47 (1997)

3. A. A. F. De Vries, E. D. Chirnside, P. J. Bredenbeek, L. A. Gravestein, M. C. Horzinek, W. J. M. Spaan Nucleic Acids Res. **18**, 3241–3247 (1990)
4. J. A. Den Boon, E. J. Snijder, E. D. Chirnside, A. A. F. de Vries, M. C. Horzinek, W. J. M. Spaan J. Virol. **65**, 2910–2930 (1991)
5. J. A. Den Boon, M. F. Kleijnen, W. J. M. Spaan, E. J. Snijder J. Virol. **70**, 4291–4298 (1996)
6. E. Van den Born, A. P. Gultyaev, E. J. Snijder RNA **10**, 424–437 (2004)
7. E. Van den Born, C. C. Posthuma, A. P. Gultyaev, E. J. Snijder J. Virol. **79**, 6312–6324 (2005)
8. G. Van Marle, J. C. Dobbe, A. P. Gultyaev, W. Luytjes, W. J. M. Spaan, E. J. Snijder Proc. Natl. Acad. Sci. USA **96**, 12056–12061 (1999)
9. A. Kheyar, G. St-Laurent, D. Archambault Virus Genes **12**, 291–295 (1996)
10. A. Kheyar, G. St-Laurent, M. Diouri, D. Archambault Can. J. Vet. Res. **62**, 224–230 (1998)
11. W. Chen, R. S. Baric J. Virol. **69**, 7529–7540 (1995)
12. M. A. Hofmann, S. D. Senanayake, D. A. Brian Proc. Natl. Acad. Sci. USA **90**, 11733–11737 (1993)
13. M. Kozak Gene **234**, 187–208 (1999)
14. G. St-Laurent, G. Morin, D. Archambault J. Clin. Microbiol. **32**, 658–665 (1994)
15. A. Kheyar, S. Martin, G. St-Laurent, P. J. Timoney, W. H. McCollum, D. Archambault Clin. Diagn. Lab. Immunol. **4**, 648–652 (1997)
16. N. Lepage, G. St-Laurent, S. Carman, D. Archambault Virus Genes **13**, 87–91 (1996)
17. J. Sambrook, E. F. Fritsch, T. Maniatis *Molecular cloning a laboratory manual*, 2nd edn. (Cold Spring Harbor Laboratory Press, Cold Spring Harbor, N.Y., 1989)
18. D. J. Anderson, G. Blobel Methods Enzymol. **96**, 111–120 (1983)
19. A. L. Glaser, A. A. F. de Vries, M. J. B. Raamsman, M. C. Horzinek, P. J. M. Rottier, in *Proceedings of the eighth international conference on equine infectious diseases*, ed. by U. Wernery, J.F. Wade, J. A. Mumford, O-R Kaaden (R & W Publications Ltd, Newmarket, England, 1998) pp. 166–176
20. J. Hierholzer, R. Killington, in *Virology methods manual*, ed. by B. W. Mahy, H. O. Kangro (Academic Press, London, 1996) pp. 38–39
21. B. A. Jameson, H. Wolf Comput. App. Biosci. **4**, 181–186 (1988)
22. D. R. Morris, A. P. Geballe Mol. Cell. Biol. **20**, 8635–8642 (2000)
23. R. Molenkamp, H. van Tol, B. C. Rozier, Y. van Der Meer, W. J. Spaan, E. J. Snijder J. Gen. Virol. **81**, 2491–2496 (2000)
24. Y.-K. Hwang, M. A. Brinton J. Virol. **72**, 4341–4351 (1998)
25. D. Archambault, M.-C. St-Louis, S. Martin Virus Genes **30**, 121–125 (2005)
26. M. Zuker, D. H. Mathews, D. H. Turner, in *RNA Biochemistry and Biotechnology*, ed. by J. Barciszewski, B. F. C. Clark (Kluwer Academic Publishers, NATO ASI Series, 1999) pp. 11–43